A Novel Calibration Method of Magnetic Compass Based on Ellipsoid Fitting

Jiancheng Fang, Hongwei Sun, Juanjuan Cao, Xiao Zhang, and Ye Tao

***Abstract*—Magnetic compass is widely used to indicate the heading of vehicle by measuring the Earth's magnetic field. However, it suffers from local magnetic interferences; thus, the calibration of the magnetic compass is very essential before it is used. The traditional calibration methods require reference information and special requirements such as keeping the magnetic compass level during calibration, which is very difficult to manage outdoor. This paper presents an efficient method for calibrating the magnetic compass without the aforementioned traditional requirements. This method is based on the fact that the error model of magnetic compass is an ellipsoid, and a constraint least-square method is adopted to estimate the parameters of an ellipsoid by rotating the magnetic compass in various (random) orientations. This method can estimate all the parameters of the error model and compensate errors caused by sensor defects, hard-iron interferences, and soft-iron interferences. Although the calibration parameters are relative values, it does not have any influence on the heading calculated. The experimental results show that this method is effective in calibrating the magnetic compass, and the heading precision of the magnetic compass acquired after calibration is better than 0.4°.**

***Index Terms*—Calibration, ellipsoid fitting, magnetic compass, magnetic interference.**

I. Introduction

THE magnetic compass is a device that indicates the heading by measuring the Earth's magnetic field. The output of the magnetic compass is continuous, available all the time, and the errors do not accumulate. Thus, it is very useful to compensate the drift of gyro and indicate the heading when the Global Positioning System is unavailable. The traditional magnetic compass which is composed of fluxgate sensors is huge and heavy. Anisotropic magnetoresistive (AMR) sensor is a full wheatstone bridge sensor that varies the resistance of the bridge in proportion to the magnetic field. It can be manufactured on silicon wafers and mounted on commercial integrated circuit packages. The magnetic compass which is made of microelectromechanical system accelerometers and AMR sensors is small, low cost, reliable, and accurate. It is widely used in a variety of applications such as aircrafts, robots, handheld navigation devices, human motion tracking, and so on [1]–[3].

Despite highly automated production process, the parameters of sensors used in the magnetic compass are different from each other. The differences mainly reflect the biases and scale factor deviations. Misalignment and nonorthogonality of the sensor axes also exist in the integrated magnetic compass. All these errors corrupt the output of magnetic compass, so it must be calibrated before use.

The nature of these errors is influenced by the local magnetic interferences such as magnetic anomalies, cabling, motors, batteries, and any ferrous or magnetic objects. These interferences can be divided into two classes: hard-iron interferences and soft-iron interferences. The hard-iron interference adds a constant bias to the sensor output. The soft-iron interference interacts with the Earth's magnetic field and generates bias that changes as the vehicle's orientation relative to the local magnetic field changes. The magnetic interference varies from place to place. Thus, it is important to account for the magnetic environment before calibration. A self-contained calibration method is required for this purpose.

There are a lot of similar methods used for calibrating magnetometers in satellites, such as the ones used for magnetic compass. A class of methods known as "attitude-dependent" methods calibrate magnetometers by comparing the measurements of magnetometers with the actual Earth's magnetic field [4], [5]. A precondition of these methods is that the vehicle orientation is known, which is difficult without the use of other high-precision navigation equipment. Another kind of methods called "attitude-independent" methods rely on the fact that the error model of magnetometers is ellipsoid to perform the calibration [6]–[8]. These methods adopt the least square or iterative algorithm to estimate the parameters of the ellipsoid. However, the iterative algorithm requires large computation and precise initial conditions. The traditional least-square algorithm cannot insure that the fitted conicoid is an ellipsoid. An advantage of the magnetic compass over magnetometer is that it does not require absolute magnitude of all components of the Earth's magnetic field. This advantage is explained mathematically in later text.

The calibration methods for the magnetic compass are few. An easy and effective calibration method called swinging algorithm is based on the fact that the heading error is a Fourier function of the heading. This algorithm is not feasible for outdoor applications because it requires a heading reference,

Manuscript received August 9, 2009; revised March 27, 2010; accepted June 29, 2010. Date of publication March 17, 2011; date of current version May 11, 2011. This work was supported in part by the Key Programs of National Natural Science Foundation of China under Grant 60736025, by the Major Programs of China National Space Administration under Grant D2120060013, and by the 973 Programs (2009CB724001, 2009CB724002). The Associate Editor coordinating the review process for this paper was Dr. Subhas Mukhopadhyay.

The authors are with the Key Laboratory of Fundamental Science for National Defense of Novel Inertial Instrument and Navigation System Technology, Beihang University, Beijing 100191, China (e-mail: fangjiancheng@buaa.edu.cn; hongweisun@aspe.buaa.edu.cn; caojuanjuan@aspe.buaa.edu.cn; taoye@aspe.buaa.edu.cn; lczx@aspe.buaa.edu.cn).

Color versions of one or more of the figures in this paper are available online at http://ieeexplore.ieee.org.

Digital Object Identifier 10.1109/TIM.2011.2115330

and the calibrated outputs are related with the magnitude of the Earth's magnetic field [9]. Another method called scalar algorithm is effective to estimate the errors of bias, scale factor, nonorthogonality, and misalignment [10], [11]. This method is also not feasible, because it requires a nonmagnetic calibration device. A third calibration method which is popularly adopted is implemented by placing the magnetic compass on a mechanical device, keeping it level and rotating it in a circle [12]. This method determines the bias and scale factor by calculating the minimum and maximum of the outputs. Although this method is convenient, it does not take into account the misalignment and nonorthogonality and is sensitive to the noise of sensors.

Vladimir presented the ellipse-fitting method to calibrate the 2-D magnetic compass [13]. This ellipse-fitting method only requires the magnetic compass to rotate horizontally and does not need any other equipment. Thus, this method is quite feasible for application in outdoor calibration process. However, for aircrafts, a 3-D magnetic compass calibration method is still needed.

To resolve all aforementioned problems, a novel calibration method based on the ellipsoid model of the 3-D magnetic field is presented in this paper. This method adopts the least-square method to estimate the error coefficients and uses these coefficients to correct the output of the magnetic compass. Moreover, a constraint condition is applied to insure the conicoid to be an ellipsoid. This method does not need any calibration device and orientation reference information during calibration. The magnetic compass can achieve high precision by this method, as long as sufficient measurements of magnetic deviations on various orientations are taken. This method is robust, convenient, and needs less computations.

The overall layout of this paper is such that Section II introduces the theoretical background of the magnetic compass. Section III gives the detailed descriptions of the error model and the calibration method for magnetic sensors. Section IV gives the error model and the calibration method for accelerometers. Section V discusses a flight simulation study to evaluate the performance of the calibration method. Section VI describes the nonmagnetic turntable experiments. Finally, the conclusion of this paper is drawn in Section VII.

II. Theoretical Background

In order to explain the calibration method clearly, first, the frames used in this paper are introduced, and these frames can transform with each other by the direction cosine matrix, Euler angles, or quaternion. The body coordinate frame (b) is fixed to the magnetic compass casing. The y_b-axis points to the forward direction and is aligned along the roll axis, the z_b-axis is upward, and the x_b-axis completes the right-handed orthogonal coordinate system (Fig. 1). The navigation coordinate frame (n) is also called the East, North, Up frame. The y_n-axis points to the local North, the x_n-axis is toward the East in the local level plane, and the z_n-axis is along the local vertical (Fig. 2). The local horizontal frame (l) is a simplified version of the navigation frame. The z_l-axis is along the local vertical, and the x_l and y_l axes are mutually orthogonal and lying in the local horizontal plane (Fig. 3).

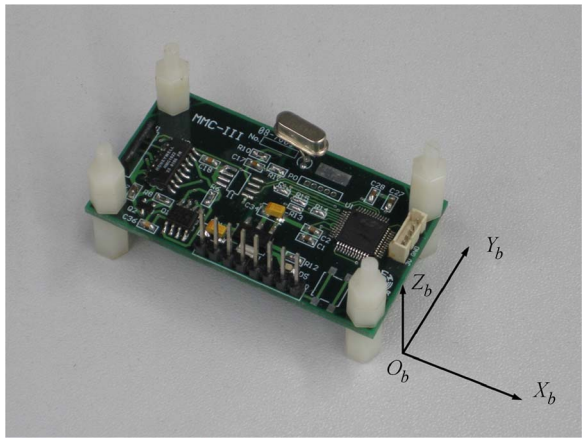

Fig. 1. Body frame.

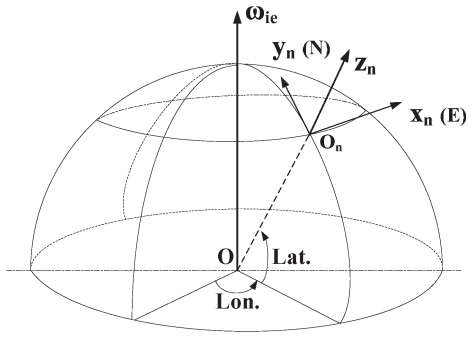

Fig. 2. Navigation frame.

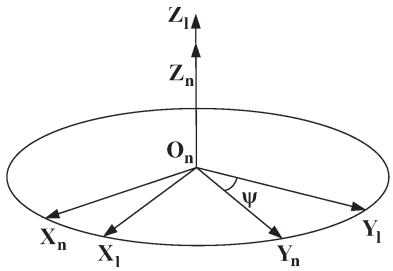

Fig. 3. Relationship between the navigation frame and the local horizontal frame.

The three-axis accelerometers are used to measure the projections of the gravity on the axis of the body frame (f_x, f_y, f_z). From these measurements, the attitude (roll-γ, pitch-θ) can be computed as

$$\gamma = -\arcsin\left(\frac{f_x}{g}\right)$$
$$\theta = \arcsin\left(\frac{f_y}{g}\right) \tag{1}$$

where g is the magnitude of the gravity.

The heading of vehicle is determined by measuring the projections of the Earth's magnetic field vector on the axis of the body frame (h_x^b, h_y^b, h_z^b). In order to calculate the heading, the measurements on the body frame must be transformed

into the local horizontal frame (h_x^l, h_y^l, h_z^l) by the following relationship:

$$\begin{bmatrix} h_x^l \\ h_y^l \\ h_z^l \end{bmatrix} = \begin{bmatrix} \cos\gamma & \sin\gamma\sin\theta & -\sin\gamma\cos\theta \\ 0 & \cos\theta & \sin\theta \\ \sin\gamma & -\sin\theta\cos\gamma & \cos\gamma\cos\theta \end{bmatrix} \begin{bmatrix} h_x^b \\ h_y^b \\ h_z^b \end{bmatrix}. \tag{2}$$

The heading (ψ) is computed as follows:

$$thead = \operatorname{arctg}\left(\frac{h_x^l}{h_y^l}\right)$$
$$\psi = \begin{cases} thead, & \left(h_x^l \geq 0, h_y^l > 0\right) \\ \pi + thead, & \left(h_y^l < 0\right) \\ 2\pi + thead, & \left(h_x^l < 0, h_y^l > 0\right) \\ \pi/2, & \left(h_x^l > 0, h_y^l = 0\right) \\ 3\pi/2, & \left(h_x^l < 0, h_y^l = 0\right). \end{cases} \tag{3}$$

According to (2) and (3), we can see that the heading is determined by the ratio of h_x^l to h_y^l. Thus, magnifying or reducing h_x^b, h_y^b, and h_z^b by k times synchronously does not affect the heading. Because the absolute magnitude of h_x^b, h_y^b, and h_z^b is not required, the calibration of the magnetic compass is easier than the magnetometer.

III. Magnetic Calibration Method

The measurements of the AMR sensors are the projections of magnetic field vector on the body axis of the magnetic compass and are denoted as $\mathbf{h}_m^b$, where the superscript b indicates the body frame. Meanwhile, the measurements of the error-free AMR sensors under no interference are denoted as $\mathbf{h}^b$. Due to the presence of the errors and interferences, $\mathbf{h}_m^b \neq \mathbf{h}^b$.

The output of AMR sensor is typically corrupted by five error sources. To describe the errors of the magnetic compass, a unified mathematical model is used as follows:

$$\mathbf{h}_m^b = \mathbf{M}_k\mathbf{M}_o\mathbf{M}_s\mathbf{h}^b + \mathbf{b} + \mathbf{n} = \mathbf{M}\mathbf{h}^b + \mathbf{b} + \mathbf{n}. \tag{4}$$

Triaxial sensor model is written in the vector form, where $\mathbf{b}$ is a constant offset that shifts the outputs of sensors. $\mathbf{M}_k$ is a 3-D diagonal matrix that accounts for the sensitivities of the individual sensors by scaling the outputs. $\mathbf{M}_o$ represents the nonorthogonality and misalignment of the triaxial AMR sensors. $\mathbf{M}_s$ is a 3×3 matrix that represents the sum of soft iron errors fixed to the body frame, which serves to scale the sensor outputs. $\mathbf{n}$ represents the noise of sensors and can be eliminated by averaging the measurements.

The calibration is the process that corrects the erroneous measured vector $\mathbf{h}_m^b$ to get the true magnetic field vector $\mathbf{h}^b$. To determine the error coefficients given in (4), the first step is to find the impact of errors on the outputs of AMR sensors.

When the magnetic compass remains stationary and only changes in direction, the magnitude of the true magnetic field $\|\mathbf{h}^b\|$ remains constant, and the locus of the true magnetic field measured $\mathbf{h}^b$ is sphere. Meanwhile, the locus of the disturbed magnetic field measured $\mathbf{h}_m^b$ is an ellipsoid, and it can be expressed as follows:

$$\|\mathbf{h}^b\|^2 = (\mathbf{h}^b)^T\,\mathbf{h}^b = \left(\mathbf{h}_m^b\right)^T\mathbf{A}\mathbf{h}_m^b - 2\mathbf{b}^T\,\mathbf{A}\mathbf{h}_m^b + \mathbf{b}^T\mathbf{A}\mathbf{b} + \tilde{\mathbf{n}} \tag{5}$$

where $\mathbf{A} = \mathbf{G}^T\mathbf{G}$, $\mathbf{G} = \mathbf{M}^{-1}$, and $\tilde{\mathbf{n}} = 2(\mathbf{h}_m^b - \mathbf{b})^T\mathbf{G}^T\mathbf{G}\mathbf{n} + (\mathbf{n})^T\mathbf{G}^T\mathbf{G}\mathbf{n}$. Even though $\mathbf{n}$ may be zero mean and Gaussian, the mean value of $\tilde{\mathbf{n}}$ $(\mathbf{E}[\tilde{\mathbf{n}}] = 2\mathbf{E}[(\mathbf{h}_m^b - \mathbf{b})^T\mathbf{G}^T\mathbf{G}\mathbf{n}] + \mathbf{E}[\|\mathbf{G}\mathbf{n}\|^2] \geq 0)$ may not. However, this method could provide the correction parameters exactly in the case that $\mathbf{n}$ goes to zero, so we ignore this problem [14].

We can see that (5) is the expression of an ellipsoid in terms of $\mathbf{h}_m^b$. In other words, the measurements $(\mathbf{h}_m^b)$ with errors are constrained to lie on an ellipsoid. Thus, the calibration of the magnetic compass is to seek ellipsoid-fitting methods to solve the coefficients of $\mathbf{G}$ and $\mathbf{b}$.

Since an ellipsoid is a kind of conicoid, (5) can be expressed as a general equation of a conicoid in the 3-D space as follows:

$$\begin{aligned} F\left(\mathbf{a}, \mathbf{h}_m^b\right) = {} & a\left(h_{mx}^b\right)^2 + b\left(h_{mx}^b\right)\left(h_{my}^b\right) + c\left(h_{my}^b\right)^2 \\ & + d\left(h_{mx}^b\right)\left(h_{mz}^b\right) + e\left(h_{my}^b\right)\left(h_{mz}^b\right) + j\left(h_{mz}^b\right)^2 \\ & + p\left(h_{mx}^b\right) + q\left(h_{my}^b\right) + r\left(h_{mz}^b\right) + s = 0 \end{aligned} \tag{6}$$

where $\mathbf{a} = [a \quad b \quad c \quad d \quad e \quad j \quad p \quad q \quad r \quad s]^T$. Moreover, the problem of fitting an ellipsoid into N data points $\mathbf{h}_m^b$ can be solved by minimizing the sum of squares of the "algebraic distances"

$$D(\mathbf{a}) = \sum_{i=1}^{N} F\left(\mathbf{a}, \mathbf{h}_m^b\right)^2. \tag{7}$$

In order to avoid the trivial solution $\mathbf{a} = \mathbf{0}_{10}$, and recognizing that any multiple of a solution $\mathbf{a}$ represents the same conicoid, the parameter vector $\mathbf{a}$ is constrained in some way. In general, this constrained problem is very difficult to solve since the Kuhn–Tucker conditions do not guarantee a solution. In order that the surface is fitted to be an ellipsoid in 3-D, Nikos proposed that the parameter vector $\mathbf{a}$ must insure the matrix $\mathbf{A}$ in (5) to be either positive or negative definite. He also presented the equivalent constrained condition for $\mathbf{a}$ [15] as follows:

Lemma [15]: $\mathbf{A}$ is positive definite or negative definite, provided that

$$\det(\mathbf{W}) > 0 \Leftrightarrow 4ac - b^2 > 0 \tag{8a}$$
$$(a + c)\det(\mathbf{A}) > 0 \tag{8b}$$

where

$$\mathbf{W} = \begin{bmatrix} a & b/2 \\ b/2 & c \end{bmatrix} \quad \mathbf{A} = \begin{bmatrix} a & b/2 & d/2 \\ b/2 & c & e/2 \\ d/2 & e/2 & j \end{bmatrix}.$$

The imposition of this inequality constraint of (8a) is difficult in general; in this case, we have the freedom to arbitrarily scale the parameters, so we may simply incorporate the scaling into the constraint and impose the equality constraint $4ac - b^2 = 1$

instead of $4ac - b^2 > 0$ [16]. $4ac - b^2 = 1$ can be expressed in the matrix form $\mathbf{a}^T\mathbf{C}\mathbf{a} = 1$ as $\mathbf{C} = \begin{bmatrix} \mathbf{C}_1 & \mathbf{C}_2 \\ \mathbf{C}_3 & \mathbf{C}_4 \end{bmatrix}$, $\mathbf{C}_1 = \begin{bmatrix} 0 & 0 & 2 \\ 0 & -1 & 0 \\ 2 & 0 & 0 \end{bmatrix}$, $\mathbf{C}_2 = 0_{3\times 7}$, $\mathbf{C}_3 = 0_{7\times 3}$, and $\mathbf{C}_4 = 0_{7\times 7}$.

In a similar work, Bookstein [17] showed that, if a quadratic constraint is set on the parameters, the minimization (7) can be solved by considering rank-deficient generalized eigenvalue system

$$\mathbf{S}^T\mathbf{S}\mathbf{a} = \lambda\mathbf{a} \tag{9}$$

where $\mathbf{S} = [\mathbf{h}^b_{m1} \quad \mathbf{h}^b_{m2} \quad \cdots \quad \mathbf{h}^b_{mN}]^T$ is called the design matrix.

Introducing the Lagrange multiplier λ and differentiating, we arrive at the system of simultaneous equations as follows:

$$\begin{matrix} \mathbf{S}^T\mathbf{S}\mathbf{a} = \lambda\mathbf{C}\mathbf{a} \\ (a+c)\det(\mathbf{A}) > 0 \end{matrix}. \tag{10}$$

In [18], it is proved that exactly one eigenvalue of (10) is positive; thus, a unique eigenvector $\mathbf{a}$ is always found using the aforementioned method, which is noniterative and thus extremely efficient.

According to (5)–(10), the error coefficients $(\mathbf{A}, \mathbf{b})$ can be determined. However, there are uncountable matrices $\mathbf{G}$ which can satisfy $\mathbf{G}^T\mathbf{G} = \mathbf{A}$. Thus, we select the x-axis of the sensors as the x-axis of the magnetic compass; thus, we can obtain the unique $\mathbf{G}$ by singular value decomposition. In this way, the calibration is achieved.

Since we scale the parameter $\mathbf{a}$, the error coefficients $(\mathbf{G}, \mathbf{b})$ estimated are relative values and not absolute ones. In other words, the $\mathbf{h}^b$ calibrated is not the absolute magnetic field vector; it may be magnified or reduced by k times. According to (2) and (3), we can see that the relative $\mathbf{h}^b$ have no influence on the heading determined.

IV. Accelerometer Calibration Method

As a kind of inertial sensors, the accelerometers are reliable, independent, and immune to environmental impact. Thus, the accelerometers only need to be calibrated once, and it is not necessary to be calibrated again when the environment changes. The primary errors of accelerometers are bias, scale factor error, nonorthogonality, and misalignment. The following equation is typically used to describe the accelerometer observation:

$$\mathbf{V}_a = \mathbf{b}_a + \mathbf{K}_a\mathbf{N}_a\mathbf{f} + \boldsymbol{\varepsilon} \tag{11}$$

where $\mathbf{V}_a = [V_{ax} \quad V_{ay} \quad V_{az}]^T$ is a 3×1 vector that represents the outputs of three accelerometers. $\mathbf{b}_a = [b_{ax} \quad b_{ay} \quad b_{az}]^T$ is the bias of accelerometers. $\mathbf{f} = [f_x \quad f_y \quad f_z]^T$ is the true specific force that we are concerned. $\mathbf{K}_a = diag[k_{ax} \quad k_{ay} \quad k_{az}]$ is the scale factor matrix. $\mathbf{N}_a$ is a 3×3 matrix which represents the impact of nonorthogonality and misalignment. $\boldsymbol{\varepsilon}$ represents the accelerometer noise and can be eliminated by averaging.

There are a lot of methods used to calibrate accelerometers. These methods are similar to each other [19], [20]. The more useful method is called multiposition calibration method. This method determines the error coefficients by comparing the outputs of accelerometers with the known projections of gravity.

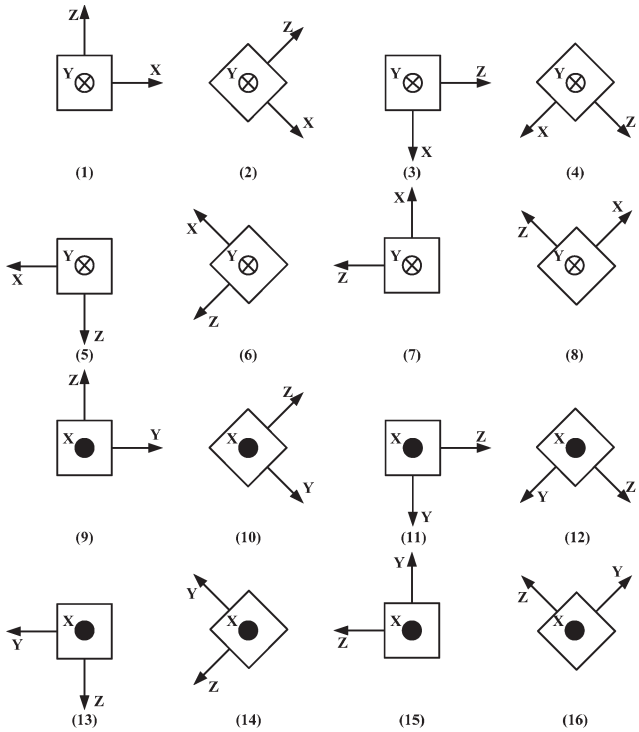

Fig. 4. 16 angular positions for the calibration of the accelerometers.

The error model of accelerometers (11) can be expressed in a matrix form as follows:

$$\begin{bmatrix} V_{ax} \\ V_{ay} \\ V_{az} \end{bmatrix} = \begin{bmatrix} n_{xx} & n_{xy} & n_{xz} & b_{ax} \\ n_{yx} & n_{yy} & n_{yz} & b_{ay} \\ n_{zx} & n_{zy} & n_{zz} & b_{az} \end{bmatrix} \begin{bmatrix} f_x \\ f_y \\ f_z \\ 1 \end{bmatrix} = \mathbf{P} \begin{bmatrix} f_x \\ f_y \\ f_z \\ 1 \end{bmatrix}. \tag{12}$$

This paper adopts 16-position method to calibrate the accelerometers. This method is comprised of three main steps. First, aligning precisely a three-axis turntable to the local horizontal frame; second, mounting the magnetic compass on the aligned turntable and aligning the body frame of the magnetic compass with the turntable by using the location pins; and finally, the third step is rotating the turntable to 16 known angular positions with respect to the local horizontal frame. The angular positions used are shown in Fig. 4.

The projections of the local gravity vector on all the 16 positions are depicted by matrix $\mathbf{L}$, shown at the bottom of the next page. This matrix is used to estimate the calibration parameters using the least-square method

In addition, the raw output of the accelerometers in voltage would be measured as a 3×16 matrix $\mathbf{U}$ which is expressed as

$$\mathbf{U} = [\mathbf{V}_1 \quad \mathbf{V}_2 \quad \cdots\cdots \quad \mathbf{V}_{16}]_{3\times 16}. \tag{14}$$

The desired coefficient matrix $\mathbf{P}$ is extracted by the least-square method as follows:

$$\mathbf{P} = (\mathbf{L}^T\mathbf{L})^{-1}\mathbf{L}^T\mathbf{U}. \tag{15}$$

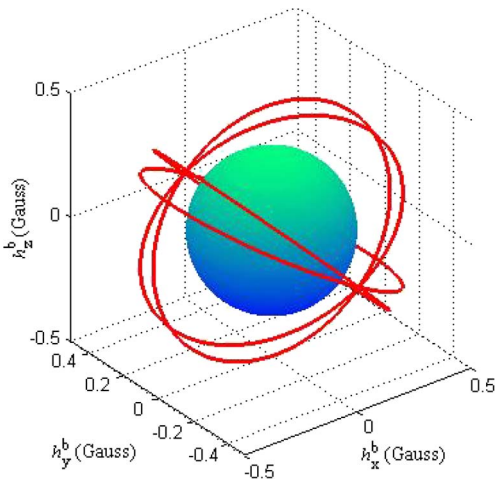

Fig. 5. Flight trajectories of simulation.

V. Simulation Study

A flight simulation study was performed to evaluate the performance of the calibration method proposed. We assumed that the magnetic field is well-proportioned, the magnitude of the magnetic field $\|\mathbf{h}^b\|$ is constant, and the magnetic compass is fixed with the aircraft flying along the trajectories shown in Fig. 5. We have devised four test trajectories each having angles with horizontal plane as 45°, −45°, 30°, and −30°, respectively. The sphere in Fig. 5 represents the magnetic field. We set the coefficients of errors caused by the magnetic interferences as shown in (16). We added a Gaussian white noise of zero mean and a variance of 0.001 G

$$\mathbf{b} = [-0.1 \quad 0.05 \quad 0.1]^T$$
$$\mathbf{M} = \begin{bmatrix} 0.8807 & -0.1875 & -0.0961 \\ -0.1875 & 1.1372 & -0.0183 \\ -0.0961 & -0.0183 & 0.5814 \end{bmatrix}. \qquad (16)$$

First, according to the local magnetic intensity and the attitude of the plane, the true magnetic field vector $\mathbf{h}^b$ and the erroneous measured vector $\mathbf{h}_m^b$ were calculated and were shown in Figs. 6 and 7, respectively.

Second, we calibrated the erroneous measurement $\mathbf{h}_m^b$ by the calibration method proposed to determine the error coefficients $\mathbf{G}$ and $\mathbf{b}$.

In the final step, we corrected the measurement vector $\mathbf{h}_m^b$, using the error coefficients calculated in the previous step, and compared the heading corrected with the actual heading. The error of the heading is shown in Fig. 8.

In Fig. 8, we noted that the method proposed in this paper was very accurate, and the standard deviation of the heading error was found as 0.15°. The more magnetic deviations we measured in different orientations, the higher precision we had achieved.

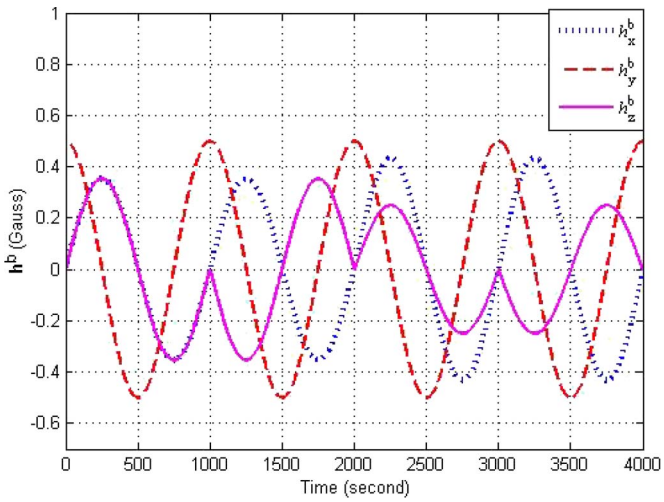

Fig. 6. True magnetic field vector $\mathbf{h}^b$.

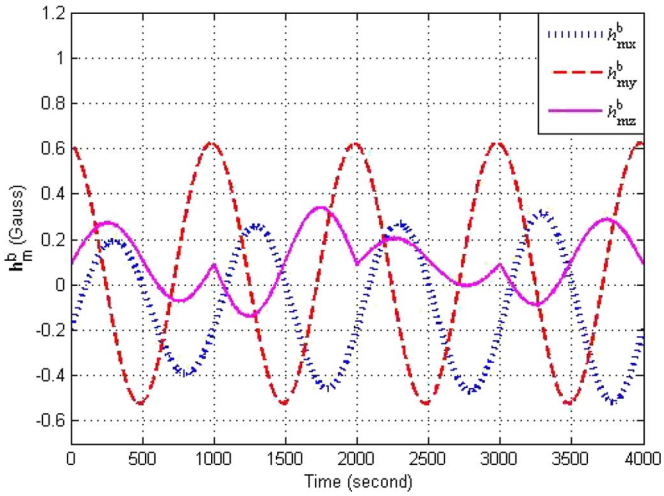

Fig. 7. Erroneous measured vector $\mathbf{h}_m^b$.

VI. Experiments

To evaluate the calibration method mentioned earlier, the nonmagnetic turntable experiment is adopted. The experiment is shown in Fig. 9. The attitude error of the nonmagnetic turntable is lower than 2′. Although this experiment was performed in a laboratory, the magnetic environment in the vicinity of the magnetic compass was not favorable.

First of all, we calibrated the accelerometer module by the method proposed in Section IV and estimated the correctional parameters listed in Table I.

$$\mathbf{L} = \begin{bmatrix} 0 & -\frac{\sqrt{2}}{2} & -1 & -\frac{\sqrt{2}}{2} & 0 & \frac{\sqrt{2}}{2} & 1 & \frac{\sqrt{2}}{2} & 0 & 0 & 0 & 0 & 0 & 0 & 0 & 0 \\ 0 & 0 & 0 & 0 & 0 & 0 & 0 & 0 & 0 & -\frac{\sqrt{2}}{2} & -1 & -\frac{\sqrt{2}}{2} & 0 & \frac{\sqrt{2}}{2} & 1 & \frac{\sqrt{2}}{2} \\ 1 & \frac{\sqrt{2}}{2} & 0 & -\frac{\sqrt{2}}{2} & -1 & -\frac{\sqrt{2}}{2} & 0 & \frac{\sqrt{2}}{2} & 1 & \frac{\sqrt{2}}{2} & 0 & -\frac{\sqrt{2}}{2} & -1 & -\frac{\sqrt{2}}{2} & 0 & \frac{\sqrt{2}}{2} \\ 1 & 1 & 1 & 1 & 1 & 1 & 1 & 1 & 1 & 1 & 1 & 1 & 1 & 1 & 1 & 1 \end{bmatrix} \qquad (13)$$

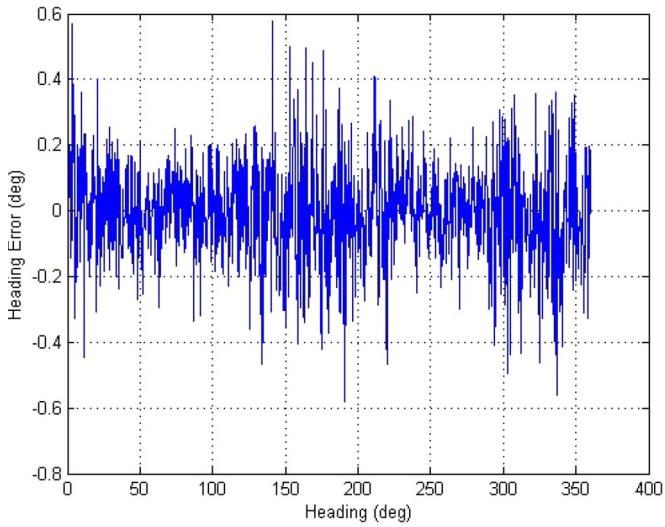

Fig. 8. Heading error of flight simulation.

Fig. 9. Nonmagnetic turntable experiment.

TABLE I
CORRECTIONAL PARAMETERS OF ACCELEROMETERS

b_{ax}	n_{xx}	n_{xy}	n_{xz}
-0.0214	0.9823	0.0169	0.0115
b_{ay}	n_{yx}	n_{yy}	n_{yz}
0.0110	-0.0231	0.9872	0.0110
b_{az}	n_{zx}	n_{zy}	n_{zz}
-0.0511	-0.0047	0.0033	1.0141

Next, the turntable was used to evaluate the attitude precision of the magnetic compass. We mounted the magnetic compass on the aligned turntable, aligned the body frame of the magnetic compass with the turntable by using the location pins, rotated the table in roll as well as in pitch by angles 0°, ±5°, ±10°, ±15°, ±20°, ±25°, ±30°, ±35°, ±40°, ±45°, ±50°, ±55°, and ±60° in separate steps. Taking the orientations of the turntable as a reference, the computed angles and angle errors of the magnetic compass were shown in Figs. 10–13, respectively.

Finally, we adopt the ellipsoid-fitting method proposed in Section III to calibrate the AMR sensor module. This procedure consists of collecting the samples of AMR sensors in various (random) orientations in homogeneous field. Then, the calibration method proposed was used to determine the correctional parameters $\mathbf{G}$ and $\mathbf{b}$. The 3-D drawing of the outputs of the AMR sensors is shown in Fig. 14. The dark sphere in Fig. 15 is the fitting of $\mathbf{h}^b$ calibrated, and the grid in Fig. 15 is the fitting of $\mathbf{h}_m^b$. The calibration parameters are listed in Table II.

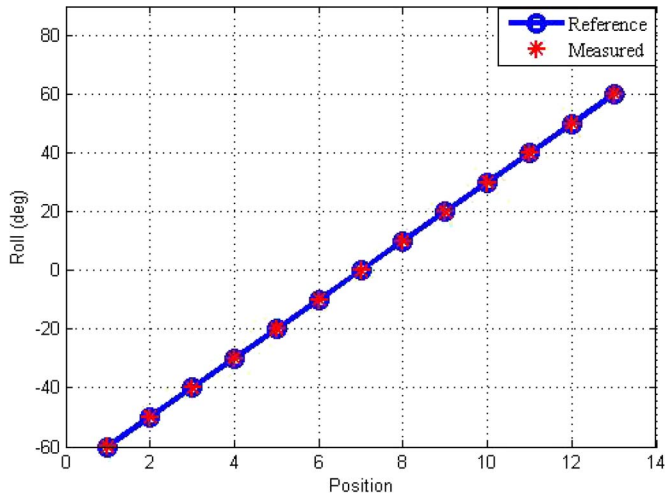

Fig. 10. Roll angle.

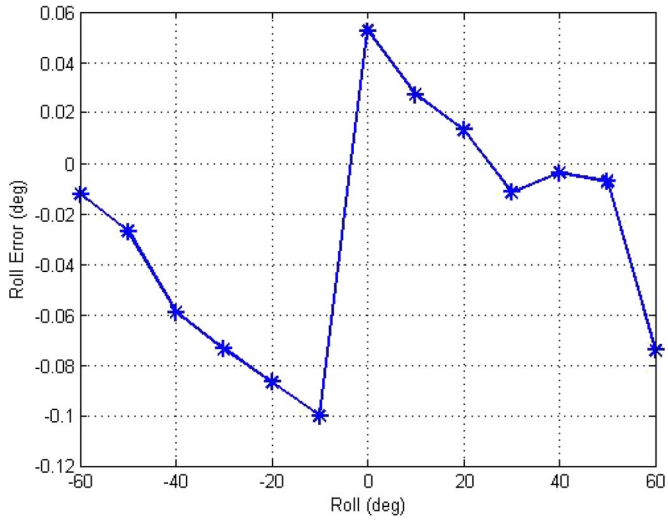

Fig. 11. Roll error of the magnetic compass.

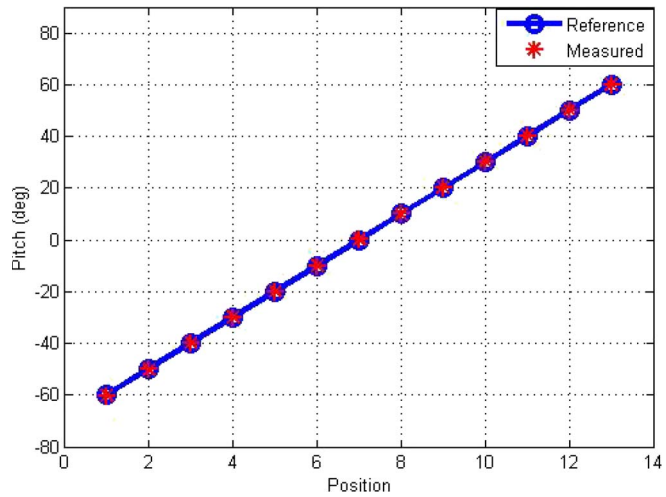

Fig. 12. Pitch angle.

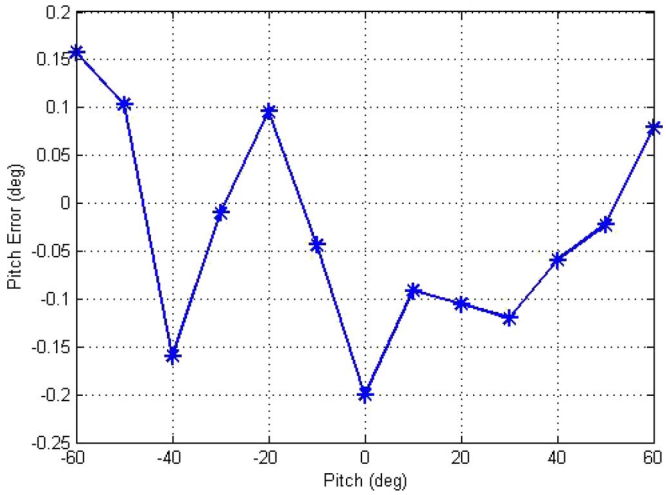

Fig. 13. Pitch error of the magnetic compass.

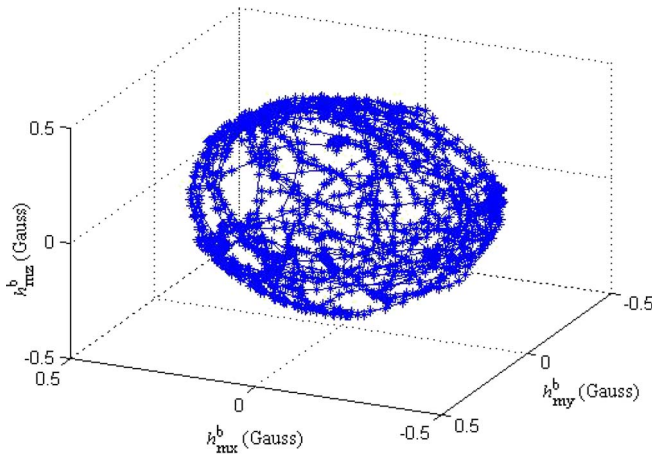

Fig. 14. Plot of recorded data from the magnetic compass.

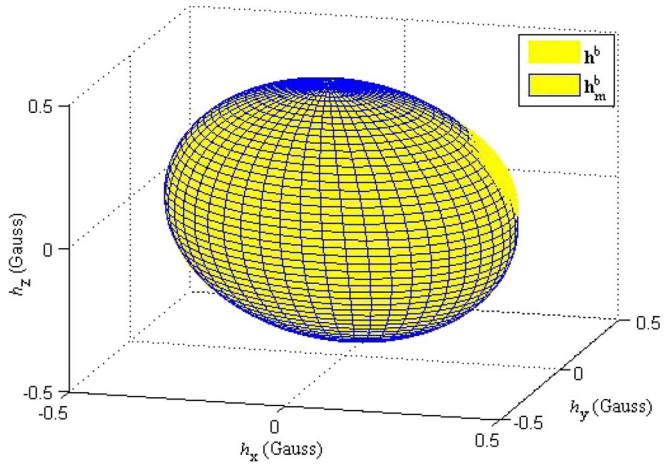

Fig. 15. Best fitting of $\mathbf{h}^b$ and $\mathbf{h}^b_m$.

TABLE II
CORRECTIONAL PARAMETERS OF AMR SENSORS

b_{mx}	**G**1,1	**G**1,2	**G**1,3
0.0007	0.9977	0.0065	0.0670
b_{my}	**G**2,1	**G**2,2	**G**2,3
-0.0294	0.0065	0.9207	0.0044
b_{mz}	**G**3,1	**G**3,2	**G**3,3
0.0169	0.0670	0.0044	0.9137

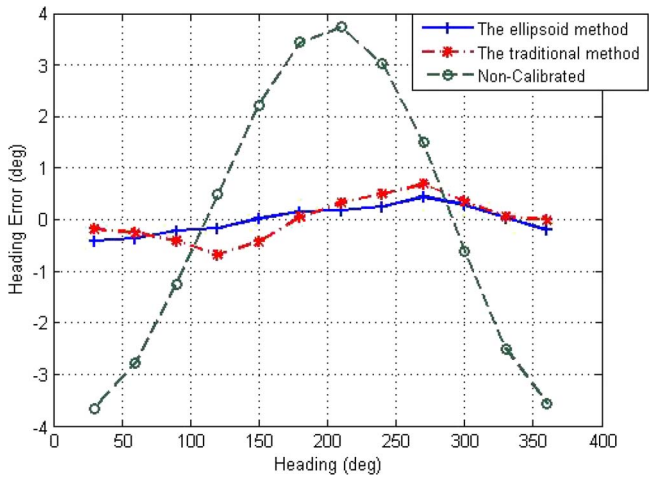

Fig. 16. Heading error of the magnetic compass in local level.

We utilized the nonmagnetic turntable aligned in the north direction to evaluate the heading precision of the magnetic compass and compared the ellipsoid-fitting calibration method with the traditional method, which is popularly used by the magnetic compass available [12]. We mounted the magnetic compass on the nonmagnetic turntable, aligned the magnetic compass with the turntable by using the location pins, and rotated in yaw by 30°, 60°, 90°, 120°, 150°, 180°, 210°, 240°, 270°, 300°, 330°, and 360°. Meanwhile, the heading outputs of the magnetic compass were collected. Taking the heading of the turntable as a reference, the heading error of the calibrated magnetic compass by the ellipsoid method was found to be 0.35° (1σ), whereas the heading error of the traditional method was 0.55° (1σ), and the heading error of the noncalibrated system is 3.59° (1σ). These results are shown in Fig. 16. In order to evaluate the effect of inclination on heading, we aligned the magnetic compass with the turntable heading 120° and turned the table in pitch by angles 0°, ±5°, ±10°, ±15°, ±20°, ±25°, ±30°, ±35°, ±40°, ±45°, ±50°, ±55°, and ±60°. Taking the heading of the turntable as a reference, the heading error of the calibrated magnetic compass by the ellipsoid method was deduced as 0.27° (1σ), whereas the heading error of the traditional method was 0.41° (1σ), and the heading error of the noncalibrated system was 2.77° (1σ). All these results are depicted in Fig. 17.

In a word, the nonmagnetic turntable experimental results showed that the ellipsoid method was more effective than the traditional method. The simulation study also showed that the ellipsoid method was effective, even though the interference was much bigger. The experimental results indicated that the heading precision of the magnetic compass was better than 0.4°.

VII. CONCLUSION

A novel calibration method based on ellipsoid fitting has been proposed and used to calibrate a three-axis magnetic compass developed in our laboratory. This calibration method can compensate the errors caused by sensor defects, hard-iron interferences, and soft-iron interferences. Although the calibrated parameters are relative values, it does not have any influence on the heading calculation. The result has been validated by

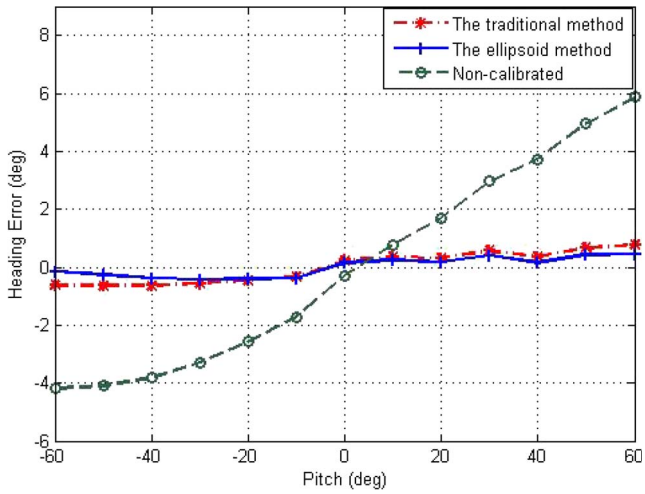

Fig. 17. Heading error of the magnetic compass during changing attitude.

performing an experiment on a nonmagnetic turntable. The experimental results show that the heading precision was better than 0.4°. This method does not require any orientation reference information, special devices, or tracks. As long as efficient measurements of magnetic deviations on various orientations are done, highly precise heading can be achieved. The system performance has shown the feasibility and high accuracy of the method.

REFERENCES

[1] V. Genovese and A. M. Sabatini, "Differential compassing helps human–robot teams navigate in magnetically disturbed environments," *IEEE Sensors J.*, vol. 6, no. 5, pp. 1045–1046, Oct. 2006.

[2] J. Bijker and W. Steyn, "Kalman filter configurations for a low-cost loosely integrated inertial navigation system on an airship," *Control Eng. Pract.*, vol. 16, no. 12, pp. 1509–1518, Dec. 2008.

[3] D. H. Lyon, "A military perspective on small unmanned aerial vehicles," *IEEE Instrum. Meas. Mag.*, vol. 7, no. 3, pp. 27–31, Sep. 2004.

[4] P. Guo, H. Qiu, and Y. Yang, "The soft iron and hard iron calibration method using extended Kalman filter for attitude and heading reference system," in *Proc. IEEE Position Location Navig. Symp.*, 2008, pp. 1167–1174.

[5] W. Koo, S. Sung, and Y. J. Lee, "Error calibration of magnetometer using nonlinear integrated filter model with inertial sensors," *IEEE Trans. Magn.*, vol. 45, no. 6, pp. 2740–2743, Jun. 2009.

[6] D. G. Egziabher, G. H. Elkaim, J. D. Powell, and B. W. Parkinson, "Calibration of strapdown magnetometers in magnetic field domain," *J. Aerosp. Eng.*, vol. 19, no. 2, pp. 87–102, Apr. 2006.

[7] C. C. Foster and G. H. Elkaim, "Extension of a two-step calibration methodology to include nonorthogonal sensor axes," *IEEE Trans. Aerosp. Electron. Syst.*, vol. 44, no. 3, pp. 1070–1078, Jul. 2008.

[8] D. Jurman, M. Jankovec, R. Kamnik, and M. Topic, "Calibration and data fusion solution for the miniature attitude and heading reference system," *Sens. Actuators A, Phys.*, vol. 138, no. 2, pp. 411–420, Aug. 2007.

[9] N. Bowditch, *The American Practical Navigator, Defense Mapping Agency*. Bethesda, MD: Hydrographic/Topographic Center, 1995, pp. 201–295.

[10] J. Vcelak, P. Ripka, J. Kubýk, A. Platil, and P. Kaspar, "AMR navigation systems and methods of their calibration," *Sens. Actuators A, Phys.*, vol. 123/124, pp. 122–128, Sep. 2005.

[11] J. Vcelak, P. Ripka, A. Platil, J. Kubik, and P. Kaspar, "Errors of AMR compass and methods of their compensation," *Sens. Actuators A, Phys.*, vol. 129, no. 1/2, pp. 53–57, May 2006.

[12] J. Yun, J. Ko, J. Lee, and J. M. Lee, "An inexpensive and accurate absolute position sensor for driving assistance," *IEEE Trans. Instrum. Meas.*, vol. 57, no. 4, pp. 864–873, Apr. 2008.

[13] V. Y. Skvortzov, H. K. Lee, S. W. Bang, and Y. B. Lee, "Application of electronic compass for mobile robot in an indoor environment," in *Proc. IEEE Int. Conf. Robot. Autom.*, Apr. 2007, pp. 2963–2970.

[14] T. Pylvanainen, "Automatic and adaptive calibration of 3D field sensors," *Appl. Math. Model.*, vol. 32, no. 4, pp. 575–587, Apr. 2008.

[15] G. Nikos and G. S. Michael, "Head detection and tracking by 2-D and 3-D ellipsoid fitting," in *Proc. IEEE Int. Conf. Comput. Graph.*, 2000, pp. 221–226.

[16] A. Fitzgibbon, M. Pilu, and R. B. Fisher, "Direct least square fitting of ellipses," *IEEE Trans. Pattern Anal. Mach. Intell.*, vol. 21, no. 5, pp. 476–480, May 1999.

[17] F. L. Bookstein, "Fitting conic sections to scattered data," *Comput. Graph. Image Process.*, vol. 9, no. 1, pp. 56–71, Jan. 1979.

[18] R. Halir and J. Flusser, "Numerically stable direct least squares fitting of ellipses," in *Proc. Int. Conf. Central Eur. Comput. Graph.*, 1998, pp. 125–132.

[19] Z. F. Syed, P. Aggarwal, C. Goodall, X. Niu, and N. El-Sheimy, "A new multi-position calibration method for MEMS inertial navigation systems," *Meas. Sci. Technol.*, vol. 18, no. 7, pp. 1897–1907, Jul. 2007.

[20] J. K. Bekkeng, "Calibration of a novel MEMS inertial reference unit," *IEEE Trans. Instrum. Meas.*, vol. 58, no. 6, pp. 1967–1974, Jun. 2009.

Jiancheng Fang was born in September 1965. He received the B.S. degree from the Shandong University of Technology (now Shandong University), Jinan, China, in 1983, the M.S. degree from Xi'an Jiaotong University, Xi'an, China, in 1988, and the Ph.D. degree from Southeast University, Nanjing, China, in 1996.

He is a Professor and the Dean of the School of Instrumentation Science and Optoelectronics Engineering, Beihang University, Beijing, China. He has authored or coauthored over 150 papers and four books. He has been granted with 35 Chinese invention patents as the first inventor. His current research mainly focuses on the attitude control system technology of spacecraft, novel inertial instrument and equipment technology, inertial navigation, and the integrated navigation technologies of aerial vehicles.

Prof. Fang has the special appointment professorship with the title of "Cheung Kong Scholar," which has been jointly established by the Ministry of Education of China and the Li Ka Shing Foundation. He is in the first group of Principal Scientists of the National Laboratory for Aeronautics and Astronautics of China. He received the first-class National Science and Technology Progress Award of China as the third contributor in 2006, the first-class National Invention Award of China as the first inventor, and the second-class National Science and Technology Progress Award of China as the first contributor in 2007.

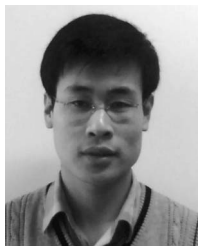

Hongwei Sun received the B.Sc. degree in automatic control from the Department of Automatic Control, Shandong University, Jinan, China, in 2003. He is currently working toward the Ph.D. degree in the School of Instrumentation Science and Optoelectronics Engineering, Beihang University, Beijing, China.

His current research interests include microinertial measurement system and micromagnetic compass design and calibration.

Juanjuan Cao received the B.Sc. degree in automatic control from the Department of Automatic Control, Nanjing University of Science and Technology, Nanjing, China, in 2000. He is currently working toward the Ph.D. degree in the School of Instrumentation Science and Optoelectronics Engineering, Beihang University, Beijing, China.

Her current research interests include inertial navigation system, integrated navigation system, and general nonlinear estimation and application.

Xiao Zhang received the B.Sc. degree in automatic control from the Department of Automatic Control, Shandong University, Jinan, China, in 2003. He is currently working toward the Ph.D. degree in the School of Instrumentation Science and Optoelectronics Engineering, Beihang University, Beijing, China.

He serves as the Technical Director of a subprogram in a Basic Research Program of the National Defense. His current interests include navigation and flight control for unmanned aerial vehicles.

Ye Tao received the B.Sc. degree in automatic control from the Department of Automatic Control, Naval Aeronautical Engineering Institute, Yantai, China, in 2001. He is currently working toward the Ph.D. degree in the School of Instrumentation Science and Optoelectronics Engineering, Beihang University, Beijing, China.

His current interests include navigation and flight control for unmanned aerial vehicles.